

2

3 **Investigating the Impact on Modeled Ozone Concentrations Using Meteorological Fields**
4 **From WRF With an Updated Four-Dimensional Data Assimilation Approach**

5 James M. Godowitch^{1,2}, Robert C. Gilliam¹, Shawn J. Roselle¹

6 ¹ Atmospheric Modeling and Analysis Division, National Exposure Research Laboratory,
7 U.S. Environmental Protection Agency, Research Triangle Park, NC 27711

8

9 **ABSTRACT**

10 The four-dimensional data assimilation (FDDA) technique in the Weather Research and
11 Forecasting (WRF) meteorological model has recently undergone an important update from the
12 original version. Previous evaluation results have demonstrated that the updated FDDA
13 approach in WRF provides more accurate wind fields aloft than the original approach,
14 particularly during the nocturnal period when low level jets are a common feature in the eastern
15 United States. Due to the importance of WRF/FDDA meteorological fields in retrospective air
16 quality applications, a modeling study with the Community Multiscale Air Quality (CMAQ) model
17 was undertaken to ascertain if the improved wind flow fields translate into better performance for
18 ozone. To undertake this objective, separate CMAQ model simulations were performed with
19 meteorological inputs generated by WRF using the original and the updated FDDA approaches
20 for a three month summer period. The evaluation effort focused on observed and modeled
21 surface ozone from a mid-morning hour (10 LDT). Comparisons of modeled results against
22 concentrations aloft from an instrumented tall tower and from available morning vertical profile
23 measurements were also examined. Surface concentrations near 10 LDT are desirable for
24 evaluating the transport process since they are often representative of ozone that has been
25 transported aloft overnight and has undergone downward entrainment in response to convective
26 mixing the following morning. Statistical results from surface observed and modeled
27 concentration pairs indicated modeled ozone from the CMAQ simulation using the updated
28 FDDA meteorology displayed smaller biases and lower absolute errors at 88% and 80% of
29 monitoring sites, respectively, in the eastern United States. The CMAQ results with the updated
30 FDDA generally exhibited smaller biases and lower absolute errors at monitoring sites across
31 the northern states than in the southeastern states. The results provide evidence that the more

32 accurate wind flows generated with the updated WRF/FDDA approach improved CMAQ model
33 performance based on the statistical results from 10 LDT ozone concentrations.

34 **Keywords:** four-dimensional data assimilation, ozone model evaluation, horizontal transport,
35 WRF, CMAQ

36 2 currently retired

37 Corresponding author: Shawn J. Roselle

38 Email: Roselle.Shawn@epa.gov

39 Phone: 1-919-541-7699

40 Fax: 1-919-541-1379

41 **1. Introduction**

42 The horizontal transport process strongly governs the spatial ozone pattern and its temporal
43 variability in air quality model simulations. Consequently, accurate three-dimensional (3-D) wind
44 fields over the entire diurnal cycle are critical to realistically simulating the horizontal distribution
45 of ozone on regional scales. Modeled wind speed and/or direction errors cause increasingly
46 larger spatial displacements in modeled ozone, which negatively impact model performance by
47 contributing to the scatter found between modeled and observed ozone concentration pairs in
48 evaluation studies. The use of four-dimensional data assimilation (FDDA) in dynamic
49 meteorological modeling has greatly improved the characterization of modeled wind flows and
50 other meteorological parameter fields in the lower troposphere for retrospective air quality
51 modeling applications (Otte, 2008a,b). The FDDA technique, or Newtonian nudging as applied
52 in a meteorological model simulation, continuously adjusts the modeled state variables of wind,
53 temperature, and moisture toward 3-D model analysis fields modified with available
54 observations and greatly reduces the accumulation of model error during the course of a
55 simulation (Seaman, 2000).

56 Developing analysis fields of winds and other meteorological variables for FDDA has recently
57 evolved as more observational data sets, especially from remote-sensing systems, have
58 become readily accessible (Gilliam et al, 2012). After Godowitch et al. (2011) found that wind
59 speeds aloft, particularly in the nocturnal low level jet and overlying residual layer were
60 underestimated in comparisons to wind profiler observations in the eastern US during nighttime
61 hours based on meteorological simulations with the existing FDDA technique, a concerted
62 model testing and evaluation effort was undertaken to develop an improved FDDA approach

63 that would generate more accurate 3-D wind fields for characterizing flows aloft during the
64 nighttime and post-sunrise periods. Based on extensive testing and evaluation with the
65 Weather Research and Forecasting (WRF) model, an updated FDDA approach that took
66 advantage of additional archived observational winds obtained by different measurement
67 platforms, as well as a key revision in the FDDA method, was adopted (Gilliam et al., 2012). In
68 particular, wind flow errors at different heights at night with the updated FDDA technique were
69 reduced compared to the original FDDA approach. Simulating the development and evolution
70 of the nocturnal low level jet, a frequent feature from the mid-Atlantic region into New England in
71 the summer (Zhang et al., 2006), is important since it can serve as a mechanism for
72 transporting pollutants hundreds of kilometers during the nocturnal period. Realistic modeling of
73 the nocturnal evolution of the wind field in the overlying residual layer of the lower troposphere
74 is also essential to accurately simulating the horizontal transport of ozone and other pollutants in
75 parts of the eastern United States during the summer season.

76 After the adoption of the updated WRF/FDDA technique, a follow up modeling study applying
77 the Community Multiscale Air Quality (CMAQ) model was necessary to investigate whether
78 improvements in simulated wind fields also translate into better model performance for ozone
79 concentrations. Therefore, photochemical simulations with the CMAQ model using
80 meteorological fields generated using WRF/FDDA with the updated and original approaches
81 were performed for a three-month summer 2002 period. Other model inputs, including
82 emissions, boundary conditions, and the model configuration remained the same in both
83 modeling scenarios. Results will consist of statistical metrics and various analyses of modeled
84 and observed surface ozone (O_3) concentration pairs from a mid-morning hour (10 local daylight
85 time (LDT)). At morning hour, it will be demonstrated that surface ozone levels reflect the
86 magnitudes of ozone found aloft which have been subjected to overnight transport in the
87 eastern United States (US). Hence, our hypothesis is that more accurate wind fields, that
88 provide a more representative characterization of the horizontal ozone distribution aloft in the
89 region, should produce improved CMAQ performance for ozone in statistical measures
90 determined with modeled and observed concentration pairs from this mid-morning hour. Further
91 information about the rationale for selecting this time to assess model results is provided in
92 section 4. The summer of 2002 was selected since additional ozone measurements aloft were
93 also available from tower and aircraft profile measurements and a broad range of O_3
94 concentrations occurred during this summer period including several high ozone episodes
95 (Godowitch et al, 2011). Additionally, testing results in Gilliam et al. (2012) revealed the updated

96 FDDA approach performed better than others for the summer 2002 episode. Comparisons of
97 modeled and observed O₃ profiles from selected experimental case studies during the summer
98 of 2002 are also examined to provide evidence in distinguishing between the ozone
99 performance of the two model simulations.

100

101 **2. Model Description and Simulation Details**

102 The CMAQ chemical transport model (version 5.0.1) with the updated Carbon Bond
103 (CB05TU) chemical mechanism including toluene chemistry (Whitten et al., 2010) was applied
104 in the simulations for this study. Other key process components of the CMAQ model base
105 configuration included the Asymmetric Convective Model version 2 (ACM2) vertical mixing
106 scheme, the Pleim-Xiu (PX) land surface model, piece-wise parabolic (PPM) horizontal
107 advection method, and deposition velocity approach for dry deposition (Byun and Schere,
108 2006).

109 The modeling domain extended beyond the continental United States and contained a 458 X
110 299 horizontal grid with a 12-km grid cell size. There were 35 vertical layers from the surface to
111 50 mb with 13 layers below 1 km. The thickness of layer 1 was \approx 20 m. The model simulations
112 spanned the three-month period from June 1 through August 31, 2002. A 10-day spin-up period
113 prior to June 1 was also simulated to minimize the effect of initial conditions. The lateral
114 boundary conditions were prescribed by concentrations generated from a Goddard Earth
115 Observing System global chemistry (GEOS-Chem) model simulation. The CMAQ model
116 configuration and these inputs were the same for both modeling scenarios.

117 Hourly meteorological parameter fields were generated by WRF version 3.3 with the same
118 12-km horizontal resolution as CMAQ. The same physics options as described in Gilliam et al.
119 (2012) were applied in both WRF simulations with the exception of a different FDDA approach.

120 The WRF/FDDA technique continuously adjusts the modeled variables with 3-D model
121 analysis fields archived from the initial conditions as well as 3-h forecasted fields of US weather
122 forecast models (Gilliam and Pleim, 2010). The original FDDA technique that was applied for
123 many years relied on routine hourly surface observations and the twice-daily rawinsonde profile
124 measurements. These measurements were introduced into a WRF utility program which
125 incorporated the observations and modified the 3-D analyses fields to produce a closer fit to the
126 observations. In the original approach, surface 2-D analysis fields were also applied for

127 adjusting modeled winds with the weighting diminishing with height over the lowest model
128 layers. Otte (2008a) and Gilliam et al. (2012) provide additional details about the original FDDA
129 technique. The updated FDDA approach described in Gilliam et al. (2012) takes advantage of
130 additional archived data sets from remotely sensing platforms, which include wind profiler
131 measurements and WSR-88 Doppler radar wind data for use in the reanalysis procedure.
132 Additionally, a revision in the FDDA technique involved the complete elimination of surface
133 analysis nudging. Both FDDA approaches applied analysis nudging to the state variables in
134 model layers above the PBL height during the entire diurnal cycle.

135 Since our CMAQ modeling study was performed independently (uncoupled mode) of the
136 WRF runs, the Meteorology-Chemistry Interface Processor (MCIP) utility program was
137 exercised with the WRF output in order to generate format-compatible meteorological data sets
138 to drive the CMAQ simulations.

139 Hourly gridded emission data sets were generated by the Sparse Matrix Operator Kernel
140 Emissions (SMOKEv2.2) processing system. Anthropogenic emissions were extracted from the
141 U.S. EPA National Emissions Inventory (NEI) for 2002 to generate gridded surface area and
142 minor point source emissions. The hourly pollutant emissions for elevated major point sources
143 were specified from Continuous Emissions Monitoring System (CEMS) data sets. Gridded on-
144 road vehicle emissions were generated by the MOBILE6.2 model. Natural surface emissions of
145 NO_x, isoprene, and other biogenic VOC species were generated by the Biogenic Emissions
146 Inventory System (BEISv3.14) model. Additional emissions from ship traffic and wildfires from
147 both periods were also included. The same emission data sets were applied in both model
148 simulations.

149 **3. Measurements and Analysis Techniques**

150 The surface ozone observations from the Air Quality System (AQS; USEPA (2002a)) network
151 sites and the Clean Air Status and Trends Network (CASTNET; USEPA (2002b)) monitoring
152 sites were matched in space and time with the modeled concentrations. While the CASTNET
153 sites are found in agricultural and forested locations at considerable distances from cities, the
154 AQS network sites are located in a variety of land uses environments within urban areas as well
155 as rural locations of the United States. Specifically, the observed O₃ at 10 LDT from each site
156 was paired against the 10 LDT hour-average modeled layer 1 concentration in the CMAQ
157 ACONC file from the grid cell containing the monitoring site location. In addition, hourly ozone
158 measurements made at 4 different heights ($z = 3$ m, 77 m, 149 m, 433 m AGL) on a TV tower

159 (i.e., WRAL-TV located near Raleigh, NC) were also available from the AQS data base since a
160 different AQS site identification number was assigned to each level. Modeled O₃ values from
161 layers containing these measurement heights were paired with the corresponding height-
162 specific hourly observations. Unfortunately, it was discovered that due to a problem with the
163 sampling tube the ozone data at the 433 m level was found to be unreliable.

164 Observed vertical O₃ profiles were obtained by a University of Maryland research aircraft at
165 selected small airport locations in the mid-Atlantic states during morning periods in conjunction
166 with an experimental field study during June and July 2002 (Castellanos et al., 2011). Details
167 about the aircraft instrumentation and sampling flights consisting of spiral ascents/descents are
168 discussed in Hains et al. (2008). The aircraft's latitude/longitude coordinates and altitude in the
169 vertical spirals were used to match up observed O₃ values with model concentrations (i.e.,
170 CMAQ 3-D CONC file) from the appropriate grid cell and vertical layer. Due to the high
171 resolution of the measurements, all observations within each model layer were averaged and
172 the mean observed values were paired with the model's layer-average concentrations that were
173 temporally interpolated to the time of the observed profile.

174 **4. Results**

175 **4.1 Examination of Ozone Aloft**

176 The time variations of mean observed ozone concentrations from two levels aloft and at the
177 surface from the WRAL-TV tower and modeled concentrations from vertical layers containing
178 the measurement heights are displayed in Figure 1. These observed and modeled results are
179 presented in separate figures since the intent is to depict the temporal behavior in the
180 observations and modeled concentrations aloft rather than to directly compare absolute
181 concentrations because the layer-average model values do not correspond to the same heights
182 as the observations. The results in Figure 1b reveal that the modeled mean values closely track
183 the temporal evolution in the observed O₃ in Figure 1a at each level. Concentrations exhibit a
184 gradual decline during the nocturnal hours after midnight, followed by a rapid rise that typically
185 occurs during the morning period. The decrease of ozone overnight is attributed to dry
186 deposition and titration with existing nitrogen oxide (NO). Weak vertical mixing within the
187 nocturnal stable boundary layer also causes the concentrations at other heights to be affected
188 by the near-surface loss processes. Once the convective mixing layer begins to grow after
189 sunrise, higher O₃ concentrations aloft are steadily mixed downward as the vertical mixing
190 process is a major contributor to the rapid increase in surface ozone concentrations during the

191 morning period (Zhang and Rao, 1999). The observed and modeled results both show that
192 surface O₃ rapidly increases and eventually attains the magnitude of concentrations at levels
193 aloft. The results indicate the concentrations at all levels are quite comparable by 10 LDT.
194 Around this time the nocturnal inversion layer has generally been eroded and the strong vertical
195 ozone gradient that had existed earlier has been eliminated. The upward extent of vertical
196 mixing finally reaches into the residual layer, where the vertical distribution of O₃ is generally
197 much less variable as will be noted later. Once the mixing into the residual layer occurs, the
198 rate of rise in surface O₃ concentrations tends to become more gradual and the role of
199 photochemical processes becomes more relevant in influencing the evolution of O₃
200 concentrations within the PBL.

201 (Insert Figure 1)

202 In contrast, vertical mixing within the well-mixed planetary boundary layer (PBL) declines in
203 the evening and winds aloft begin to accelerate which can transport the leftover O₃ contained
204 within the residual layer considerable distances during the nocturnal period. Vukovich and
205 Scarborough (2005) have given a thorough description of the nocturnal evolution of ozone
206 transport. During the summer months, the residual layer extends from the top height of the
207 surface-based nocturnal inversion layer (e.g., 300-500 m AGL) to the preceding day's PBL
208 height (e.g., 1 500 - 2 500 m AGL). The ozone concentrations within the residual layer
209 generally exhibit little change during the nocturnal period and early morning hours, however, the
210 wind flow differences between these simulations is expected to produce notable spatial
211 displacements in the horizontal ozone pattern aloft. An example case in Figure 2a depicts the
212 modeled spatial O₃ pattern after an extended period of nocturnal transport. High O₃
213 concentrations aloft in the mid-morning (i.e., 10 LDT) are evident in various areas of the eastern
214 United States in these CMAQ results using the updated FDDA meteorology which were also
215 evident in the surface layer 1 O₃ field by this time. In fact, notable high ozone plumes are
216 apparent in the mid-Atlantic (MA) states, Ohio River Valley (ORV) region and northeastern (NE)
217 states. Figure 2b shows notable O₃ differences at this time between the two model simulations
218 of up to ± 20 ppb in the vicinity of the high concentration plumes where large horizontal
219 gradients exist in this case. A generally southwesterly (SW) wind flow, a common pattern
220 occurring in the eastern United States during summer (Godowitch et al., 2011), prescribed the
221 orientation of notable O₃ plumes. In particular, the higher O₃ areas and O₃ differences along
222 the NE coast and MA regions primarily exhibit the signatures of major urban plumes, while
223 major point sources in the ORV region (Godowitch et al., 2008) contribute to O₃ variations in the

224 vicinity of the ORV and further downwind into northern NE in this case. These spatial
225 concentration differences were a common feature in these model simulations and these
226 displacements are attributed to speed and direction variations in the wind flows generated by
227 the original and updated FDDA approaches. It is apparent that in some areas in Figure 2b there
228 are also small O₃ differences of a few ppb.

229 (Insert Figure 2)

230 The lack of spatially-dense and temporally-resolved observed ozone profile measurements
231 has greatly limited attempts to distinguish which ozone pattern is closer to reality. However, the
232 results in Figure 3 give some evidence that the CMAQ O₃ aloft using the updated meteorology
233 provides better overall agreement to the morning observed profile at this central Virginia site
234 during this field study case than the modeled profile generated using the original FDDA
235 meteorology, especially in the residual layer above about 500 m. Mean observed O₃ from the
236 aircraft spirals and modeled profiles were also determined from 30 sites over 10 morning cases.
237 Results in Figure 4a indicate the mean modeled profiles are quite similar to each other and both
238 model results are very comparable to O₃ concentrations aloft in the observed mean profile. The
239 small differences between the modeled mean ozone profiles from these simulations suggest
240 that many of the aircraft profiles were obtained at sites in areas where ozone was rather
241 spatially uniform, which does not help to distinguish between the model results. Figure 4a
242 reveals that both modeled results overestimate observed mean values in the lowest few
243 hundred meters, which will also be assessed from analysis of the surface observed/modeled
244 pairs.

245 (Insert Figure 3)

246 Additional results of grouping the modeled O₃ values between 500-1 500 m over 10 ppb
247 intervals of observed O₃ are shown in Figure 4b. At lower observed concentrations, these
248 modeled results tend to overestimate observed ozone, while at the highest concentrations the
249 modeled results slightly underestimated observed values. Both modeled results appear to
250 mimic evaluation results of afternoon maximum ozone concentrations at the surface (Appel et
251 al. 2007; Mao et al., 2010), which might not be unexpected since ozone aloft in the morning can
252 be traced back to the previous day's ozone levels. Figure 4b also indicates the modeled results
253 using the updated FDDA meteorology exhibit slightly less variability at the higher concentration
254 levels. Next, comparisons of ozone from 10 LDT from the broader spatial coverage and higher

255 density of surface monitoring sites are expected to provide a better opportunity to distinguish
256 between the model performance of these simulations.

257 (Insert Figure 4)

258 **4.2 Comparative Results of Modeled and Observed Surface Ozone Concentrations**

259 The statistical metrics shown in Table 1 were determined from observed and modeled 10
260 LDT ozone pairs from AQS and CASTNET monitoring sites located in the eastern United States
261 over the 92 days of the modeling period. The results revealed that the model simulation using
262 the updated FDDA meteorology exhibited better model performance with a smaller mean bias
263 (MB) by about 20% and a lower mean absolute error (MAE) by about 8% than those for the
264 model results using the original FDDA meteorology for each group of sites.

265 (Insert Table 1)

266 An additional metric examined for this study was the frequency factor (Fp) defined as the
267 percentage of cases that each model simulation value was closer to an observation than the
268 other simulation result. To determine Fp, the absolute difference ($|M - O|$) between each
269 modeled and observed O₃ concentration at 10 LDT was determined and the simulation result
270 exhibiting the smaller absolute difference was selected. Table 1 reveals that the CMAQ results
271 with the updated FDDA meteorology were more frequently closer to observations with an Fp of
272 58% versus only 42% for simulation results using the original FDDA meteorology. A typical
273 case showing which model value was closer to the observed 10 LDT O₃ value at each AQS site
274 is depicted in Figure S1. In this case, the modeled results using the updated FDDA
275 meteorology more accurately simulated observed values at 62% of the sites and it's modeled
276 values were especially in better agreement at numerous sites along the northeast urban corridor
277 stretching from Washington, DC to Connecticut. A notable result was that Fp for the updated
278 FDDA simulation was higher on each day than Fp for the results using the original FDDA
279 meteorology.

280 Since differences in the bulk statistical metrics were somewhat modest, further analysis was
281 performed in an effort to identify more definitive differences from site-specific statistical metrics.
282 A comparison of MAE between both simulations in Figure 5 reveals that the modeled results
283 using the updated FDDA meteorology exhibited less error at over 80% of AQS sites with MAEs
284 lower by 10% or more at sites where higher model errors existed. The spatial distribution of
285 MAE from the simulation using the updated FDDA meteorology is shown in Figure S2. Lower

286 model errors generally occurred at sites in the northern states, while higher MAEs were more
287 often found in the southeastern states. This result is also borne out in Table 1 which indicates a
288 lower MAE for the AQS/NE site group than in the overall AQS/EUS sites that also contains the
289 southeastern sites.

290 (Insert Figure 5)

291 The site-specific MB results are compared between these simulations in Figure 6. Results
292 indicate that MB values for model results from the updated FDDA meteorology were less than
293 those for the simulation results using the original FDDA meteorology at 88% of the sites. The
294 spatial distribution of MB is displayed in Figure S3 at all AQS sites from the updated FDDA
295 simulation results. Small positive model biases are generally found at sites in the northern
296 states and underestimates by the model occur at relatively few locations. On the other hand,
297 the highest positive biases, where the largest model overestimates of 10 LDT O₃ occurred, at
298 sites in the southeastern states. Additionally, a closer examination of the difference in MB
299 between these simulations in Figure 7 indicates that MB for modeled results using the updated
300 FDDA meteorology was quite close to the bias in the other simulation at AQS sites in the
301 southeastern US, while exhibiting much lower MB values at the vast majority of sites in the
302 northern areas of the domain. A possible cause for the greater error and more bias in both
303 model simulations in the southeastern region of the domain is overestimated ozone boundary
304 conditions. Wind flows in the summer more frequently transport air westward across the
305 Atlantic Ocean or from the Gulf of Mexico into the southeastern US and modeled O₃ can be
306 overestimated since chemical mechanisms currently do not account for various halogen species
307 emissions over large water bodies that may destroy O₃ and dry deposition velocities need to be
308 increased over water bodies in CMAQ (Sarwar et al, 2014).

309 (Insert Figure 6)

310 (Insert Figure 7)

311 **5. Summary**

312 In this model evaluation study, CMAQ simulations were conducted with meteorological data
313 sets generated by WRF using the original and updated FDDA approaches to investigate
314 whether more accurate wind fields from the latter produces better model performance for mid-
315 morning ozone in the eastern United States. The rationale for focusing on 10 LDT ozone was
316 that concentrations at this time reflect transported ozone which in an evaluation could better

317 isolate the impact of differences in wind fields on model performance. Statistical results based
318 on modeled and observed 10 LDT ozone pairs revealed that modeled results with the updated
319 FDDA meteorology exhibited less bias and smaller absolute errors at a large majority of
320 monitoring sites. Comparative results of morning ozone profiles indicated that modeled
321 concentrations closely matched observed values in the residual layer. Comparisons of modeled
322 ozone against tower measurements showed that CMAQ replicated the temporal variation of
323 ozone after midnight and through the morning period. The notable positive model ozone bias in
324 the southeastern US may be attributable to overestimated ozone in the southern boundary
325 conditions, which deserves further investigation.

326 **Acknowledgements**

327 The advice and encouragement of ST Rao, our former division director, during the initial phase
328 of this modeling study is gratefully appreciated. The authors extend their thanks to the
329 University of Maryland RAMMPP program for allowing access to the aircraft data archive. The
330 U.S. Environmental Protection Agency through its Office of Research and Development funded
331 and managed the research described here. Although it has been subjected to Agency review
332 and clearance, it does not necessarily reflect the views and policies of the Agency.

333 **Supporting Material Available**

334 Example of modeled ozone concentration closest to observed values (Figure S1), mean
335 absolute error at AQS sites (Figure S2), and mean bias at AQS sites (Figure S3). This
336 information is available free of charge via the Internet at <http://www.atmospolres.com>.

337

338 **References**

- 339 Appel, K.W., Gilliland, A.B., Sarwar G., Gilliam R.C., 2007. Evaluation of the Community
340 Multiscale Air Quality (CMAQ) model version 4.5: Sensitivities impacting model
341 performance. Part I – Ozone. *Atmospheric Environment*, 41, 9603-9615.
- 342 Byun, D.B., and Schere, K.L., 2006. Review of the governing equations, computational
343 algorithms, and other components of the Models3 Community Multiscale Air Quality
344 (CMAQ) modeling system. *Applied Mechanics Review*, 55, 51-77.
- 345 Castellanos, P., Marufu, L.T., Doddridge, B.G., Taubman, B.F., Schwab, J.J., Hains, J.C.,
346 Ehrman, S.H., and Dickerson, R.R., 2011. Ozone, oxides of nitrogen, and carbon
347 monoxide during pollution events over the eastern United States: An evaluation of
348 emissions and vertical mixing. *Journal of Geophysical Research*, 116,
349 doi:10.1029/2010JD014540.

350 Gilliam, R.C., Pleim, J.E., 2010. Performance assessment of new land surface and planetary
351 boundary layer physics in the WRF-ARW. *Journal of Applied Meteorology and*
352 *Climatology*, 49, 760-774.

353 Gilliam, R.C., Godowitch, J.M., Rao, S.T., 2012. Improving the horizontal transport in the lower
354 troposphere with four dimensional data assimilation. *Atmospheric Environment*, 53, 186-
355 201.

356 Godowitch, J.M., Gilliland, A.B., Draxler, R.R., Rao, S.T., 2008: Modeling assessment of point
357 source NO_x emission reductions on ozone air quality in the eastern United States.
358 *Atmospheric Environment*, 42, 87-100.

359 Godowitch, J.M., Gilliam, R.C., Rao, S.T., 2011. Diagnostic evaluation of ozone production and
360 horizontal transport in a regional photochemical air quality modeling system. *Atmospheric*
361 *Environment*, 45, 3977-3987.

362 Hains, J.C., Taubman, B.F., Thompson, A.M., Stehr, J.W., Marufu, L.T., Doddridge, B.G.,
363 Dickerson, R.R., 2008. Origins of chemical pollution derived from mid-Atlantic aircraft
364 profiles using a cluster technique. *Atmospheric Environment*, 47, 1727-1741.

365 Mao, H., Chen, M., Hegarty, J.D., Talbot, R.W., Koerner, J.P., Thompson, A.M., Avery, M.A.,
366 2010. A comprehensive evaluation of seasonal simulations of ozone in the northeastern
367 US during summers of 2001-2005. *Atmospheric Chemistry and Physics*, 10, 9-27.

368 Otte, T.L., 2008a. The impact of nudging in the meteorological model for retrospective air quality
369 simulations. Part I: evaluation against national observation networks. *Journal of Applied*
370 *Meteorology and Climatology*, 47, 1853-1867.

371 Otte, T.L., 2008b. The impact of nudging in the meteorological model for retrospective air quality
372 simulations. Part II: evaluating collocated meteorological and air quality observations. *J.*
373 *Applied Meteorology and Climatology* 47, 1868-1887.

374 Sarwar, G., Xing, J., Godowitch, J., Schwede, D., Mathur, R., 2014. Impact of RACM2, halogen
375 chemistry and updated ozone deposition velocity on hemispheric ozone predictions. 33rd
376 International Technical Meeting, Miami, FL, Springer Publishers.

377 Seaman, N.L., 2000. Meteorological modeling for air quality assessments. *Atmospheric*
378 *Environment*, 34, 2231-2259.

379 USEPA, 2002a. <http://www.epa.gov/ttn/airs/airsaqs/detaildata>, accessed in June 2013.

380 USEPA, 2002b. <http://www.epa.gov/castnet>, accessed in June 2013.

381 Vukovich, F.M., Scarborough, J., 2005. Aspects of ozone transport, mixing, and chemistry in the
382 greater Maryland area. *Atmospheric Environment*, 39, 7008-7019.

383 Whitten, G.Z., Heo, G., Kimura, Y., McDonald-Buller, E., Allen, D., Carter, W., Yarwood, G.,
384 2010. *Atmospheric Environment*, 44, 5346-5355.

- 385 Zhang, D., Zhang, S., Weaver, S.J., 2006. Low-level jets over the mid-Atlantic states: Warm
386 season climatology and a case study. *Journal of Applied Meteorology and Climatology*, 45,
387 194-209.
- 388 Zhang, J., Rao, S.T., 1999. The role of vertical mixing in the temporal evolution of ground-level
389 ozone concentrations. *Journal of Applied Meteorology*, 38, 1674-1691.

390

Figure Captions

391 Figure 1. a) Hourly variation of ozone at 3 levels on the WRAL-TV tower near Raleigh, NC and
392 b) hourly mean modeled ozone from 3 corresponding layers containing the measurement levels.
393 Measurements heights are imbedded within model layers 1, 3, and 5, respectively, and layer 8
394 is near 400 m AGL. Data are missing at specific hours in the tower measurements due to
395 routine instrument calibrations.

396 Figure 2. a) Spatial ozone pattern from the updated simulation on June 11 at 10 LDT in layer 10
397 (\approx 600 m AGL) and b) ozone differences (updated and original).

398 Figure 3. Observed and modeled O₃ profiles at a central Virginia site (Louisa, VA) at 0915 LDT
399 on June 11.

400 Figure 4. a) Mean observed and modeled mid-morning ozone profiles are derived from June
401 and July 2002 cases. Dashed lines represent $\pm 1\sigma$ from the mean observed values. b) Modeled
402 original (red) and updated (blue) ozone based on values from 500-1 500 m AGL in all morning
403 profiles.

404 Figure 5. Comparison of mean absolute error (MAE) between the CMAQ simulation results at
405 individual AQS sites. Updated MAE is lower than the original MAE at 80% of all sites.

406 Figure 6. Comparison of mean bias (MB) between the updated and original simulation results at
407 individual AQS sites. MB from the updated simulation is lower at 88% of sites.

408 Figure 7. Difference in mean bias values (updated - original) at AQS sites. Negative values
409 indicate less bias in the simulation results with updated FDDA meteorology.

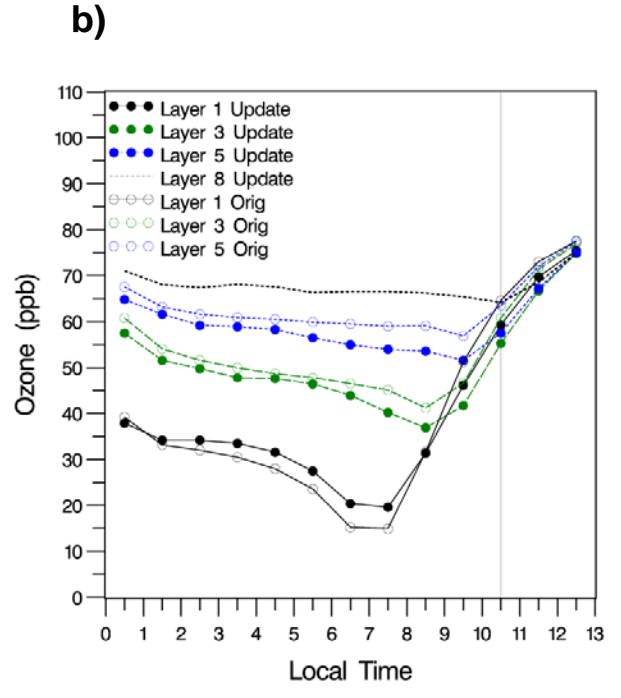
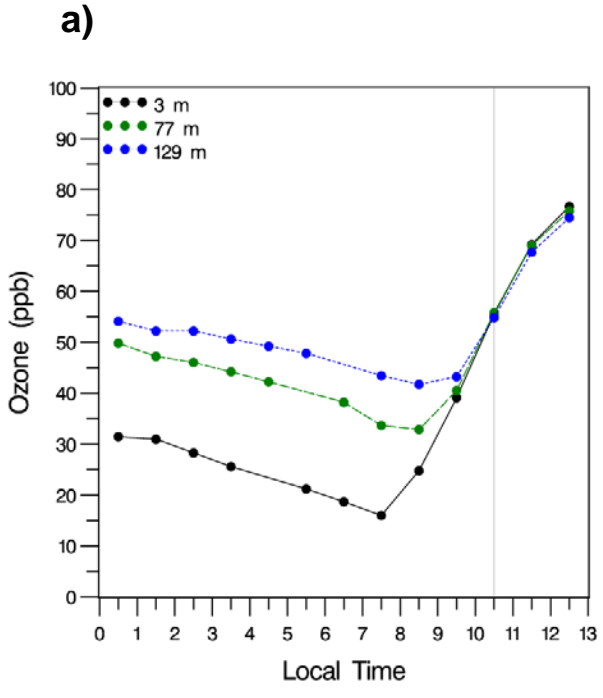
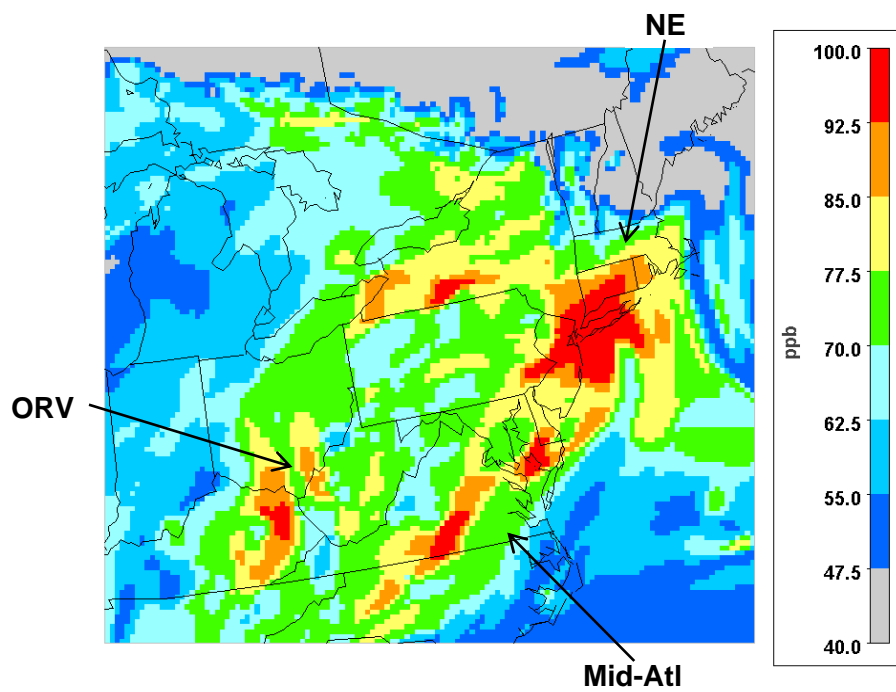


Figure 1

a)



b)

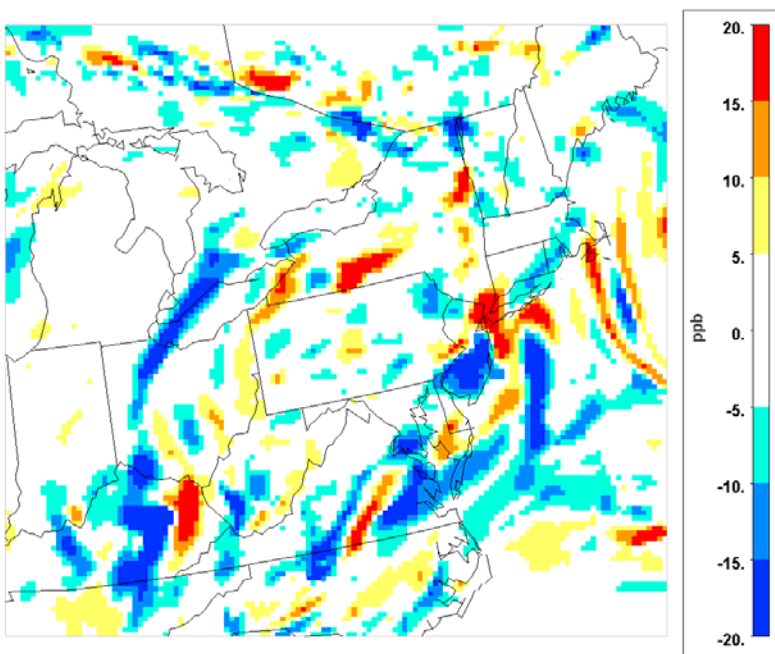


Figure 2.

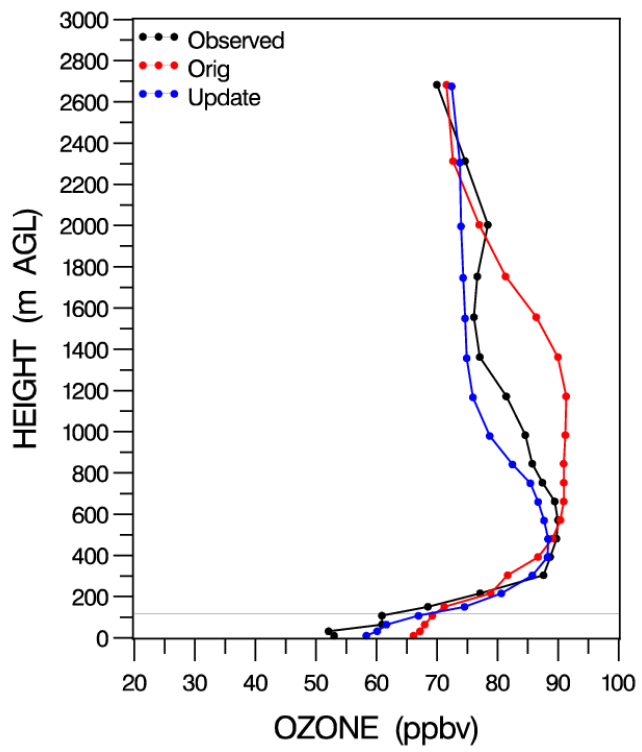
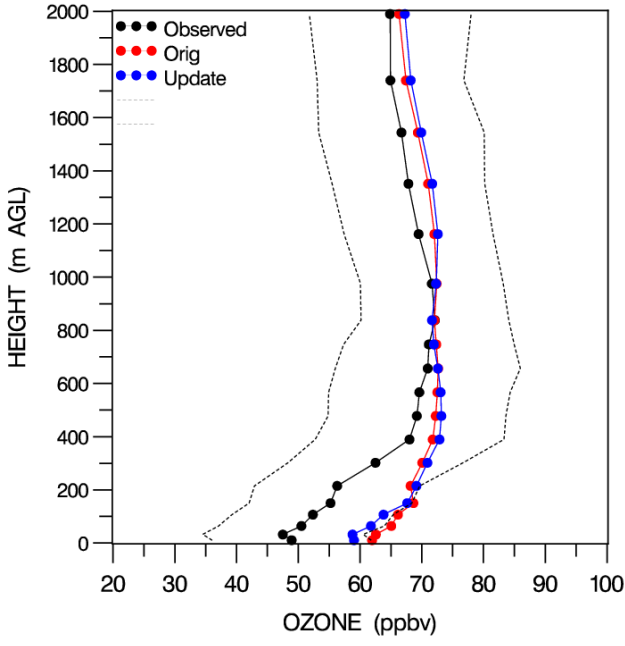


Figure 3.

a)



b)

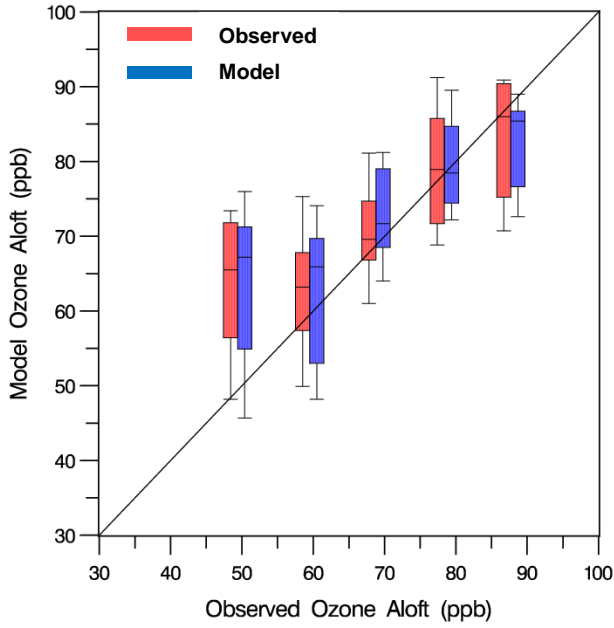


Figure 4.

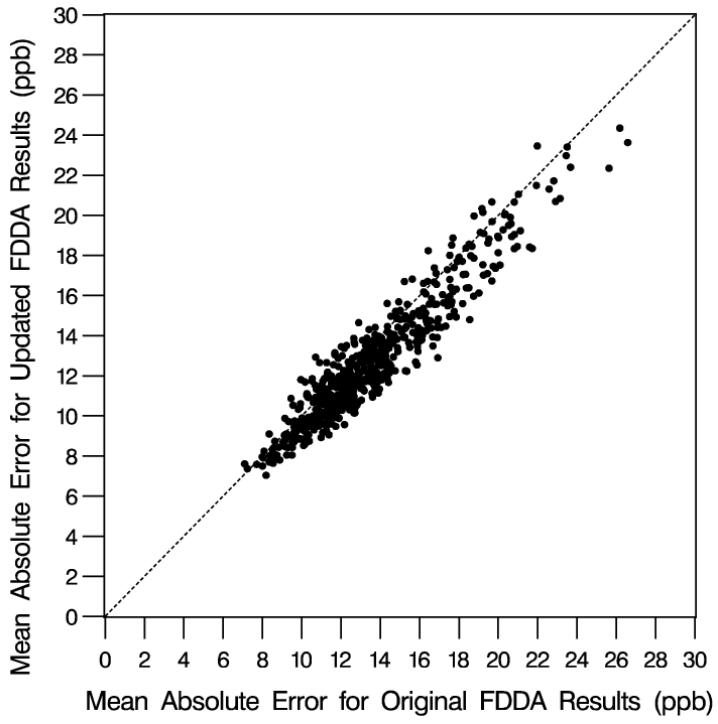


Figure 5.

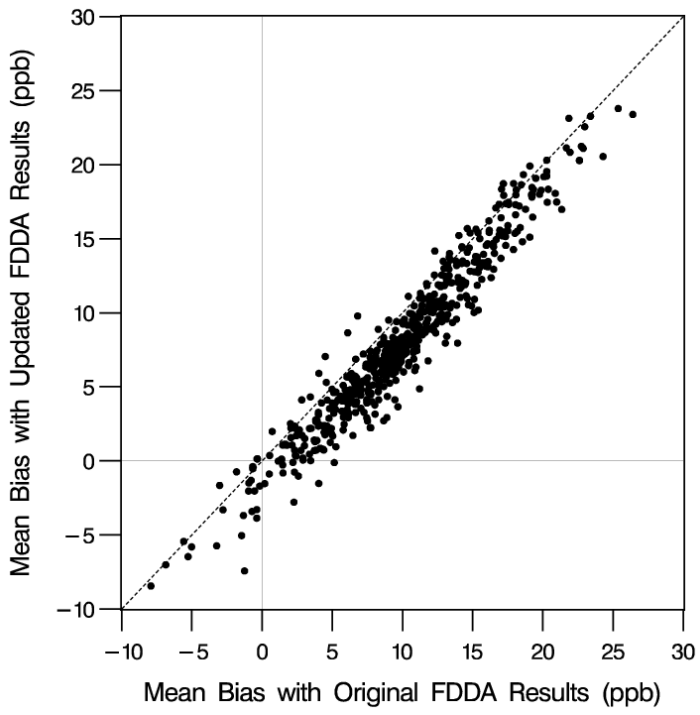


Figure 6.

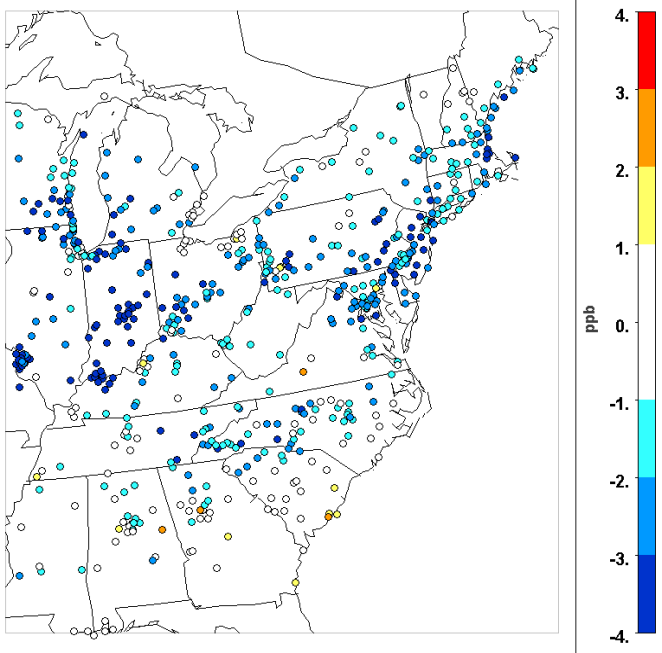


Figure 7.

Table 1. Statistical Results for Observed and Modeled 10 LDT Ozone Concentrations

Sites	N ^a	Mean Obs (ppbv)	Mean Model		MB ^d		MAE ^e		Fp ^f	
			S1 ^b (ppbv)	S2 ^c (ppbv)	S1 (ppbv)	S2 (ppbv)	S1 (ppbv)	S2 (ppbv)	S1 (%)	S2 (%)
AQS/EUS ^g	37731	40.3	50.1	48.2	9.8	7.9	13.5	12.6	42	58
AQS/NE ^h	13402	41.4	49.6	47.5	8.2	6.1	12.4	11.5	41	59
CNET ⁱ	2892	42.1	52.9	51.1	10.8	9.0	13.3	12.5	42	58

a N = number of observed and modeled pairs

b S1 = simulation with original FDDA meteorology

c S2 = simulation with updated FDDA meteorology

d MB = mean bias

e MAE = mean absolute error

f Fp = percentage of cases that results of a simulation were closer to observations

g EUS = 619 sites in 27 states east of the Mississippi River

h NE = sites in 11 northeastern states

i CNET = 34 CASTNET eastern sites

James M. Godowitch, Robert C. Gilliam, and Shawn J. Roselle

Investigating the Impact on Modeled Ozone Concentrations Using Meteorological Fields From WRF with and Updated Four-Dimensional Data Assimilation Approach

Captions for Supporting Figures

Figure S1. Example illustrates which modeled ozone concentration (blue; updated, red; original) is closer to the observed value at AQS sites on June 11 at 10 LDT.

Figure S2. Mean absolute error at AQS sites from the CMAQ simulation results using the updated FDDA meteorology.

Figure S3. Mean bias (MB) at AQS sites from the updated FDDA simulation.

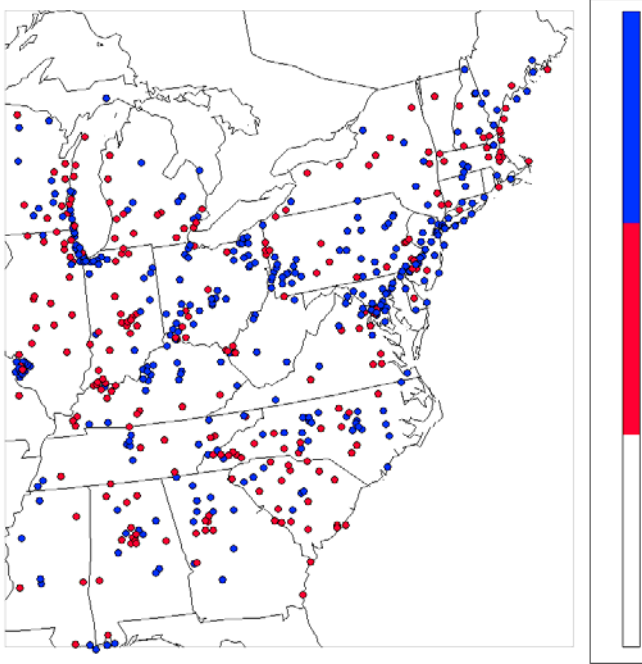


Figure S1.

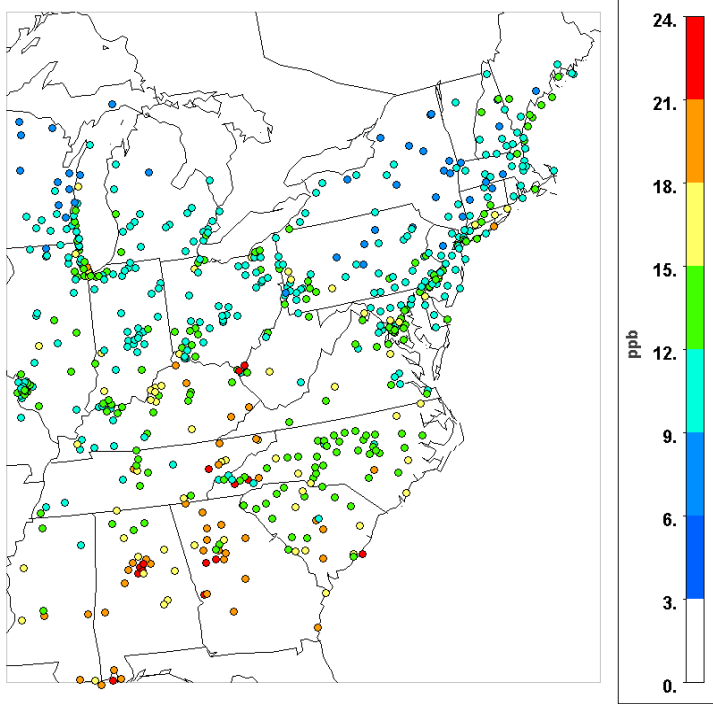


Figure S2.

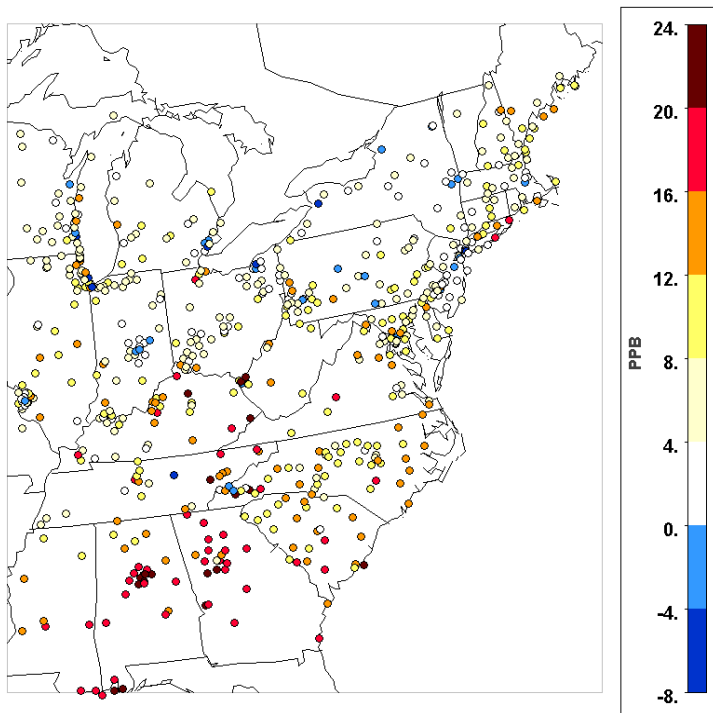


Figure S3.